

Total-energy minimization of few-body electron systems in the real-space finite-difference scheme

This article has been downloaded from IOPscience. Please scroll down to see the full text article.

2009 J. Phys.: Condens. Matter 21 064231

(<http://iopscience.iop.org/0953-8984/21/6/064231>)

View [the table of contents for this issue](#), or go to the [journal homepage](#) for more

Download details:

IP Address: 129.252.86.83

The article was downloaded on 29/05/2010 at 17:47

Please note that [terms and conditions apply](#).

Total-energy minimization of few-body electron systems in the real-space finite-difference scheme

Hidekazu Goto and Kikuji Hirose

Department of Precision Science and Technology and Applied Physics, Graduate School of Engineering, Osaka University, Suita, Osaka 565-0871, Japan

E-mail: goto@prec.eng.osaka-u.ac.jp

Received 20 July 2008, in final form 15 October 2008

Published 20 January 2009

Online at stacks.iop.org/JPhysCM/21/064231

Abstract

A practical and high-accuracy computation method to search for ground states of few-electron systems is presented on the basis of the real-space finite-difference scheme. A linear combination of Slater determinants is employed as a many-electron wavefunction, and the total-energy functional is described in terms of overlap integrals of one-electron orbitals without the constraints of orthogonality and normalization. In order to execute a direct energy minimization process of the energy functional, the steepest-descent method is used. For accurate descriptions of integrals which include bare-Coulomb potentials of ions, the time-saving double-grid technique is introduced. As an example of the present method, calculations for the ground state of the hydrogen molecule are demonstrated. An adiabatic potential curve is illustrated, and the accessibility and accuracy of the present method are discussed.

1. Introduction

Even with recent achievements which have resulted from a lot of studies on the electronic structure calculations [1–17], theoretical and methodological studies for simulations of many-electron systems which yield more accurate results without relying on approximations are very important and interesting issues for computational physics, chemistry and biology [18–24]. In addition, since high-performance computing facilities are available in the present day, rigorous or exact electronic structure calculations are feasible in studies of many-electron systems.

In the present study, a simple and practical method to search for ground states of few-electron systems is introduced on the basis of the real-space finite-difference (RSFD) scheme [25, 26]. As a many-electron wavefunction, a linear combination of Slater determinants is employed, and the total-energy functional is described with overlap integrals of one-electron orbitals. The key point of the present method is the direct energy minimization (DEM) of the total-energy functional [27–30] based on the variational principle *without the constraints of orthogonality and normalization* on the one-electron orbitals. Thus, this method can be a practical

computational tool to search for the ground states without using conventional self-consistent field techniques [31]. In the Hartree–Fock (HF) theory [32], by way of comparison, a single Slater determinant is employed as a many-electron wavefunction, and the electron–electron interactions are calculated through the self-consistent mean-field. In particular, the HF method requires the constraints of orthogonality and normalization on the one-electron basis set; as a compensation for such constraints, enormously many Slater determinants are required for high-accuracy computations [33].

In order to apply the present method to practical use, we give a simple and accessible description of the steepest-descent (SD) algorithm. For high-accuracy calculations of ionic systems, the time-saving double-grid (DG) technique [34, 35] is also introduced. A simple formulation for dealing with the systems including nuclei whose potentials have singularities is described, and successful results in which the numerical calculation errors caused by the RSFD scheme are removed by the DG technique are illustrated.

As an example of the present method, calculations for the ground-state energy of the hydrogen molecule are demonstrated. An adiabatic potential curve is illustrated and the availability of the present method is discussed.

It will be shown that the evaluated equilibrium interatomic distance and total energy are in good agreement with the exact results [36, 37].

The rest of the paper is organized as follows. In section 2, the total-energy functional for a many-electron system is introduced as a function of the overlap integrals of non-orthogonal one-electron basis functions using a linear combination of Slater determinants. In section 3 the DEM method using the SD algorithm without the constraints of orthogonality and normalization on the one-electron basis set is proposed, and in section 4 the DG technique for high-accuracy numerical calculations of ionic systems is presented. Finally, the method is applied to calculations of the ground state of the hydrogen molecule as an example of two-electron systems in section 5. A summary of the present study is given in section 6.

2. Representation of the total-energy functional

An expression of the total-energy functional for an N -electron system is introduced here using Slater determinants as a many-electron wavefunction. The N -electron wavefunction $\Psi(\mathbf{r}_1, \mathbf{r}_2, \dots, \mathbf{r}_N)$ is expanded in terms of non-orthogonal Slater determinants as follows:

$$\Psi(\mathbf{r}_1, \mathbf{r}_2, \dots, \mathbf{r}_N) = \sum_{A=1}^L \Phi^A(\mathbf{r}_1, \mathbf{r}_2, \dots, \mathbf{r}_N). \quad (1)$$

Here, \mathbf{r}_i denotes the position of the i th electron and L denotes the number of Slater determinants. Spin indices are ignored for simplicity. $\Phi^A(\mathbf{r}_1, \mathbf{r}_2, \dots, \mathbf{r}_N)$ denotes the A th Slater determinant, as given by

$$\begin{aligned} \Phi^A(\mathbf{r}_1, \mathbf{r}_2, \dots, \mathbf{r}_N) &= \frac{1}{\sqrt{N!}} \begin{vmatrix} \phi_1^A(\mathbf{r}_1) & \phi_2^A(\mathbf{r}_1) & \cdots & \phi_N^A(\mathbf{r}_1) \\ \phi_1^A(\mathbf{r}_2) & \phi_2^A(\mathbf{r}_2) & \cdots & \phi_N^A(\mathbf{r}_2) \\ \vdots & \vdots & \ddots & \vdots \\ \phi_1^A(\mathbf{r}_N) & \phi_2^A(\mathbf{r}_N) & \cdots & \phi_N^A(\mathbf{r}_N) \end{vmatrix}, \quad (2) \end{aligned}$$

with $\phi_i^A(\mathbf{r})$ being non-orthogonal and unnormalized one-electron basis functions.

The overlap integral matrix S^{AB} is defined by

$$S^{AB} = \begin{bmatrix} s_{11}^{AB} & s_{12}^{AB} & \cdots & s_{1N}^{AB} \\ s_{21}^{AB} & s_{22}^{AB} & \cdots & s_{2N}^{AB} \\ \vdots & \vdots & \ddots & \vdots \\ s_{N1}^{AB} & s_{N2}^{AB} & \cdots & s_{NN}^{AB} \end{bmatrix}, \quad (3)$$

where the elements s_{ij}^{AB} denote the overlap integrals between the one-electron basis functions, i.e.,

$$s_{ij}^{AB} = \int d\mathbf{r} \phi_i^{A*}(\mathbf{r}) \phi_j^B(\mathbf{r}). \quad (4)$$

Thus, we have the total-energy functional E which is expressed explicitly using the overlap integral matrix as [31]

$$E = \frac{\sum_{A=1}^L \sum_{B=1}^L (\langle \hat{H}_0^{AB} \rangle + \langle \hat{H}_I^{AB} \rangle)}{\sum_{A=1}^L \sum_{B=1}^L |S^{AB}|}, \quad (5)$$

where $\langle \hat{H}_0^{AB} \rangle$ and $\langle \hat{H}_I^{AB} \rangle$ are the matrix elements of the Hamiltonian,

$$\hat{H}_0 = \sum_{n=1}^N \left(-\frac{1}{2} \Delta_n + V(\mathbf{r}_n) \right) \quad (6)$$

and

$$\hat{H}_I = \sum_{n=1}^N \sum_{n'=1}^N \frac{1}{|\mathbf{r}_n - \mathbf{r}_{n'}|}, \quad (7)$$

respectively. Here, $V(\mathbf{r})$ stands for an external potential. These matrix elements $\langle \hat{H}_0^{AB} \rangle$ and $\langle \hat{H}_I^{AB} \rangle$ are represented as [31]

$$\langle \hat{H}_0^{AB} \rangle = |S^{AB}| \sum_{i=1}^N \sum_{j=1}^N [(S^{AB})^{-1}]_{ji} h_{ij}^{AB} \quad (8)$$

and

$$\begin{aligned} \langle \hat{H}_I^{AB} \rangle &= \frac{1}{2} |S^{AB}| \sum_{I=1}^N \sum_{J=1}^N [(S^{AB})^{-1}]_{JI} \\ &\times \sum_{i=1}^{N-1} \sum_{j=1}^{N-1} [(S_{[I,J]}^{AB})^{-1}]_{ji} \int d\mathbf{r} \varphi_{IJ}^{AB}(\mathbf{r}) [W_{[I,J]}^{AB}(\mathbf{r})]_{ij}, \quad (9) \end{aligned}$$

where

$$h_{ij}^{AB} = \int d\mathbf{r} \phi_i^{A*}(\mathbf{r}) \left(-\frac{1}{2} \Delta + V(\mathbf{r}) \right) \phi_j^B(\mathbf{r}). \quad (10)$$

Here, $[(S^{AB})^{-1}]_{ji}$ denotes the element of the j th row and i th column of the matrix $(S^{AB})^{-1}$. $S_{[I,J]}^{AB}$ and $W_{[I,J]}^{AB}(\mathbf{r})$ represent $(N-1)$ -dimensional matrices constructed by eliminating the I th row and the J th column from the matrices S^{AB} and $W^{AB}(\mathbf{r})$, respectively, and the matrix $W^{AB}(\mathbf{r})$ is defined as

$$W^{AB}(\mathbf{r}) = \begin{bmatrix} w_{11}^{AB}(\mathbf{r}) & w_{12}^{AB}(\mathbf{r}) & \cdots & w_{1N}^{AB}(\mathbf{r}) \\ w_{21}^{AB}(\mathbf{r}) & w_{22}^{AB}(\mathbf{r}) & \cdots & w_{2N}^{AB}(\mathbf{r}) \\ \vdots & \vdots & \ddots & \vdots \\ w_{N1}^{AB}(\mathbf{r}) & w_{N2}^{AB}(\mathbf{r}) & \cdots & w_{NN}^{AB}(\mathbf{r}) \end{bmatrix}, \quad (11)$$

where

$$w_{ij}^{AB}(\mathbf{r}) = \int d\mathbf{r}' v(\mathbf{r} - \mathbf{r}') \varphi_{ij}^{AB}(\mathbf{r}'), \quad (12)$$

and

$$\varphi_{ij}^{AB}(\mathbf{r}) = \phi_i^{A*}(\mathbf{r}) \phi_j^B(\mathbf{r}). \quad (13)$$

Here, $v(\mathbf{r} - \mathbf{r}')$ is the electron–electron interaction between electrons at positions \mathbf{r} and \mathbf{r}' , i.e.,

$$v(\mathbf{r} - \mathbf{r}') = \frac{1}{|\mathbf{r} - \mathbf{r}'|}. \quad (14)$$

Let us estimate the computational cost of equation (9). Without respect to the number of employed Slater determinants L , the calculation costs for S^{AB} , $|S^{AB}|$ and $(S^{AB})^{-1}$ are $N^2 \times N_{\text{grid}}$, N^3 and N^3 , respectively. Here, N_{grid} denotes the number of grid points in space. Then $(S_{[I,J]}^{AB})^{-1}$ requires N^5 , and the cost for $W_{[I,J]}^{AB}(\mathbf{r})$ is $N^2 \times N_{\text{grid}}$ [31]. As a result, the dominant cost for computing equation (5) turns out to be $L^2 \times N^4 \times N_{\text{grid}}$, since $N_{\text{grid}} \gg N$ in the present case of few-body electron systems.

3. Direct energy minimization (DEM) using the steepest-descent (SD) method

In order to search for ground states of target systems based on the variational principle, the DEM method [27–30] is carried out for the total-energy functional equation (5) without restricting the orthogonality and normalization to the one-electron basis set within the framework of the RSFD scheme [25, 26]. In the DEM process, an arbitrary initial state $\phi_j^A(\mathbf{r}_i)^{(\text{initial})}$ is prepared. The SD direction $\xi_j^A(\mathbf{r}_i) \equiv -\delta E/\delta\phi_j^{A*}(\mathbf{r}_i)$ is given by

$$\xi_j^A(\mathbf{r}_i) = -\sum_{B=1}^L \left(\frac{\delta(\langle \hat{H}_0^{AB} \rangle + \langle \hat{H}_I^{AB} \rangle)}{\delta\phi_j^{A*}(\mathbf{r}_i)} - E \frac{\partial |S^{AB}|}{\partial\phi_j^{A*}(\mathbf{r}_i)} \right) / \sum_{A=1}^L \sum_{B=1}^L |S^{AB}|. \quad (15)$$

In the SD procedure, the one-electron wavefunctions are updated iteratively by

$$\phi_j^A(\mathbf{r}_i)^{(\text{new})} = \phi_j^A(\mathbf{r}_i)^{(\text{old})} + \alpha_j^A \xi_j^A(\mathbf{r}_i) \quad (i, j = 1, 2, \dots, N), \quad (16)$$

where α_j^A is the acceleration parameter, which is determined by

$$\frac{d}{d\alpha_j^A} E(\Psi^*(\mathbf{r}_1, \mathbf{r}_2, \dots, \mathbf{r}_N)^{[A,j]}, \Psi(\mathbf{r}_1, \mathbf{r}_2, \dots, \mathbf{r}_N)^{[A,j]}) = 0. \quad (17)$$

Here, $\Psi(\mathbf{r}_1, \mathbf{r}_2, \dots, \mathbf{r}_N)^{[A,j]}$ represents a many-electron wavefunction in which the A th Slater determinant is replaced by

$$\begin{aligned} \Phi^A(\mathbf{r}_1, \mathbf{r}_2, \dots, \mathbf{r}_N)^{[j]} &\equiv \|\vec{\phi}_1^A \vec{\phi}_2^A \dots \vec{\phi}_N^A\|^{[j]} \\ &\equiv \|\vec{\phi}_1^A \vec{\phi}_2^A \dots (\vec{\phi}_j^A + \alpha_j^A \xi_j^A) \dots \vec{\phi}_N^A\| \\ &= \|\vec{\phi}_1^A \vec{\phi}_2^A \dots \vec{\phi}_N^A\| + \alpha_j^A \|\vec{\phi}_1^A \vec{\phi}_2^A \dots \vec{\phi}_N^A\|^{(j)} \end{aligned} \quad (18)$$

with

$$\vec{\phi}_i^A \equiv [\phi_i^A(\mathbf{r}_1)\phi_i^A(\mathbf{r}_2) \dots \phi_i^A(\mathbf{r}_N)]^t \quad (19)$$

being a column vector constructing the Slater determinant $\|\vec{\phi}_1^A \vec{\phi}_2^A \dots \vec{\phi}_N^A\|$.

Here,

$$\|\vec{\phi}_1^A \vec{\phi}_2^A \dots \vec{\phi}_N^A\|^{(j)} \equiv \|\vec{\phi}_1^A \vec{\phi}_2^A \dots \vec{\phi}_{j-1}^A \vec{\xi}_j^A \vec{\phi}_{j+1}^A \dots \vec{\phi}_N^A\|, \quad (20)$$

and

$$\vec{\xi}_j^A \equiv [\xi_j^A(\mathbf{r}_1)\xi_j^A(\mathbf{r}_2) \dots \xi_j^A(\mathbf{r}_N)]^t. \quad (21)$$

Equation (17) gives a quadratic equation with respect to α_j^A ,

$$(Y_H X_S - X_H Y_S)(\alpha_j^A)^2 + 2(X_H Z_S - Z_H X_S)\alpha_j^A + (Z_H Y_S - Y_H Z_S) = 0. \quad (22)$$

Here,

$$X_H = \int d\Omega \left[\prod_{p=1}^N \phi_p^{A*}(\mathbf{r}_p) \right]^{(j)} (\hat{H}_0 + \hat{H}_I) \|\vec{\phi}_1^A \vec{\phi}_2^A \dots \vec{\phi}_N^A\|^{(j)}, \quad (23)$$

$$Y_H = \sum_{B=1}^N \int d\Omega \left[\prod_{p=1}^N \phi_p^{A*}(\mathbf{r}_p) \right]^{(j)} (\hat{H}_0 + \hat{H}_I) \|\vec{\phi}_1^B \vec{\phi}_2^B \dots \vec{\phi}_N^B\|, \quad (24)$$

$$Z_H = \sum_{A=1}^L \sum_{B=1}^L (\langle H_0^{AB} \rangle + \langle H_I^{AB} \rangle), \quad (25)$$

$$X_S = \int d\Omega \left[\prod_{p=1}^N \phi_p^{A*}(\mathbf{r}_p) \right]^{(j)} \|\vec{\phi}_1^A \vec{\phi}_2^A \dots \vec{\phi}_N^A\|^{(j)}, \quad (26)$$

$$Y_S = \sum_{B=1}^N \int d\Omega \left[\prod_{p=1}^N \phi_p^{A*}(\mathbf{r}_p) \right]^{(j)} \|\vec{\phi}_1^B \vec{\phi}_2^B \dots \vec{\phi}_N^B\|, \quad (27)$$

and

$$Z_S = \sum_{A=1}^L \sum_{B=1}^L |S^{AB}|, \quad (28)$$

where

$$\begin{aligned} \left[\prod_{p=1}^N \phi_p^{A*}(\mathbf{r}_p) \right]^{(j)} &\equiv \phi_1^{A*}(\mathbf{r}_1)\phi_2^{A*}(\mathbf{r}_2) \dots \phi_{j-1}^{A*}(\mathbf{r}_{j-1})\xi_j^{A*}(\mathbf{r}_j) \\ &\quad \times \phi_{j+1}^{A*}(\mathbf{r}_{j+1}) \dots \phi_N^{A*}(\mathbf{r}_N), \end{aligned} \quad (29)$$

and $\int d\Omega$ represents the integration with respect to the coordinates \mathbf{r}_i for all electrons, i.e.,

$$\int d\Omega \equiv \int_{\mathbf{r}_1} \int_{\mathbf{r}_2} \dots \int_{\mathbf{r}_N} d\mathbf{r}_1 d\mathbf{r}_2 \dots d\mathbf{r}_N. \quad (30)$$

One of the two solutions of equation (22), which gives lower total energy, is adopted for updating the wavefunction through equation (16). Iterations of the SD process for all of the one-electron wavefunctions lead to a numerical solution of the ground state. In the procedure of the DEM, numerical calculations of the kinetic energy term are performed in the RSFD scheme [25, 26]. In cases searching for excited states, initial electronic states will converge to the excited states when the DEM procedure is performed under a constraint of the orthogonality with the ground state.

4. Time-saving double-grid (DG) technique

In the RSFD formalism [25, 26], the numerical values of wavefunctions, charge densities and potentials are defined only on discrete grid points in space. Therefore, total-electron energies fluctuate depending on the positions of the atoms relative to the grid points. This fluctuation is not induced by physical phenomena but by numerical errors. Although this problem can be avoided by reducing the grid spacing, the usage of denser-grid points results in a substantial increase of the computational workload. However, this problem has been excellently conquered by the time-saving DG technique [34, 35], in which coarse and dense grids are used simultaneously. In the previous studies, the DG technique is implemented only for systems in which pseudopotentials are adopted as atomic potentials. In the present study, we apply the DG technique to systems in which the bare atomic potential of the nucleus

$$V_v(r) = -\frac{Z_v}{r} \quad (31)$$

is employed, where Z_v denotes the charge of the v th nucleus. Now the bare atomic potential $V_v(r)$ is separated into two parts by the error function $\text{erf}(a_v r)$ as

$$V_v(r) = V_v^{(\text{soft})}(r) + V_v^{(\text{hard})}(r), \quad (32)$$

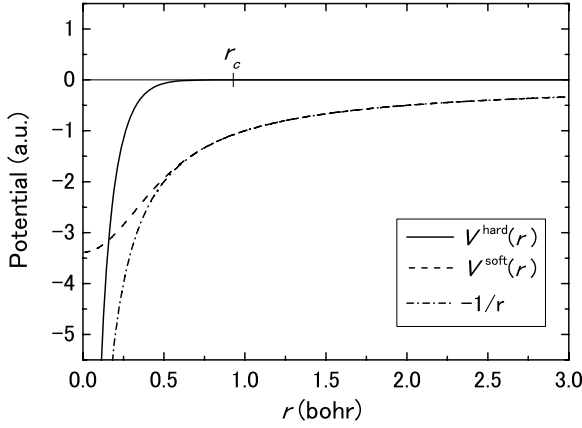


Figure 1. Illustration of the atomic potential in the DG technique. The solid and dashed lines represent the hard part $V_v^{(\text{hard})}(r)$ and soft part $V_v^{(\text{soft})}(r)$ in equation (32), respectively. The atomic charge $Z_v = 1$ and $a_v = 3.0$ are adopted. A cut-off radius r_c of 0.928 is indicated in the condition that $V_v^{(\text{hard})}(r_c)$ becomes less than 1.0×10^{-4} .

where

$$V_v^{(\text{soft})}(r) = -\frac{Z_v}{r} \text{erf}(a_v r), \quad (33)$$

and

$$V_v^{(\text{hard})}(r) = -\frac{Z_v}{r} \{1 - \text{erf}(a_v r)\}. \quad (34)$$

Here, a_v denotes the parameter to rule the locality of the hard-part potential $V_v^{(\text{hard})}(r)$. The potentials $V_v^{(\text{soft})}(r)$ and $V_v^{(\text{hard})}(r)$ are illustrated in figure 1 in the case of $a_v = 3.0$. The hard part $V_v^{(\text{hard})}(r)$ attenuates rapidly with r so that dense-grid points are defined only inside of the cut-off radius r_c . On the other hand, the soft part $V_v^{(\text{soft})}(r)$ smoothly varies so that it is defined only on coarse-grid points.

Let us consider the one-dimensional case for instance. In order to calculate integrals including the hard part $V_v^{(\text{hard})}(x)$ with high accuracy, it should be evaluated using the numerical values on dense-grid points as

$$\int V_v^{(\text{hard})}(x) \phi_j(x) dx = \sum_{k=-n_d N_{\text{grid}}/2}^{n_d N_{\text{grid}}/2-1} V_{v,k}^{(\text{hard})} \phi_{j,k}^{(\text{dense})} \delta x. \quad (35)$$

Here, $\phi_{j,k}^{(\text{dense})}$ is the numerical value of the j th one-electron wavefunction $\phi_j(x)$ on the k th dense-grid point, and n_d and δx denote the number of dense-grid points per coarse-grid spacing and the dense-grid spacing, respectively. For convenience, N_{grid} is chosen as an even integer.

Using the linear interpolation, $\phi_{j,k}^{(\text{dense})}$ is expressed in terms of the values at the coarse-grid points $\phi_{j,K}$ and $\phi_{j,K+1}$ by

$$\begin{aligned} \phi_{j,k}^{(\text{dense})} &= \frac{\delta X - (x_k - X_K)}{\delta X} \phi_{j,K} \\ &+ \frac{\delta X - (X_{K+1} - x_k)}{\delta X} \phi_{j,K+1}, \end{aligned} \quad (36)$$

where X_K and x_k represent the coordinates of the K th coarse-grid point and k th dense-grid point, respectively, and δX denotes the coarse-grid spacing. Inserting equation (36)

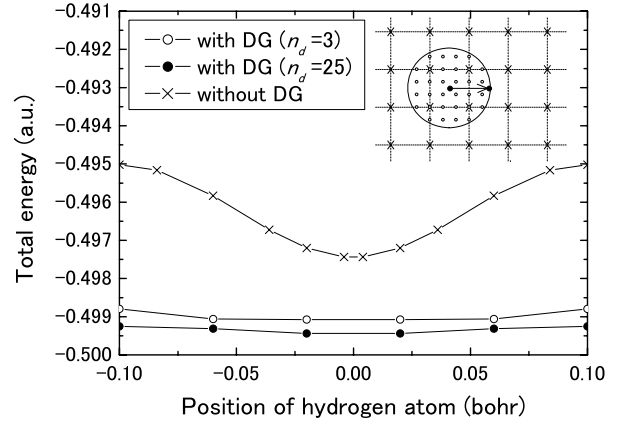


Figure 2. Variation of the total energy of the hydrogen atom as a function of the position of the nucleus with the choice of the coarse-grid spacing $\delta X = 0.2$ bohr. The hydrogen atom is positioned along the straight line shown in the inset in which the coarse-grid points and the dense-grid points are indicated by crosses and open circles, respectively. Two cases in which the number of dense-grid points per coarse-grid spacing, n_d , are shown is 3 and 25. The result without using the DG technique is also illustrated for comparison. Good stability of the DG technique can be seen.

into (35), we have the following expression for the integral using only numerical values on coarse-grid points [34, 35]:

$$\int V_v^{(\text{hard})}(x) \phi_j(x) dx = \sum_{K=-N_{\text{grid}}/2}^{N_{\text{grid}}/2-1} w_{v,K} \phi_{j,K} \delta X, \quad (37)$$

where

$$w_{v,K} = \sum_{s=-n_d}^{n_d} \frac{\delta X - |X_K - x_{n_d K+s}|}{n_d \delta X} V_{v,n_d K+s}^{(\text{hard})}, \quad (38)$$

which is a weight factor defined only on coarse-grid points. Note that numerical values of $w_{v,K}$ can be calculated and stored in advance.

Thus, for N_{ion} ionic systems, equation (10) can be expressed in the RSFD scheme as

$$h_{ij}^{AB} = \sum_K \phi_{i,K}^{A*} \left[\left(-\frac{1}{2}\Delta\right) + \sum_{v=1}^{N_{\text{ion}}} (V_{v,K}^{(\text{soft})} + w_{v,K}) \right] \phi_{j,K}^B \delta X. \quad (39)$$

The kinetic energy term in equation (39) is treated by means of the finite-difference formulae for the Laplacian [25, 26].

In order to illustrate the advantage of the DG technique, the total-electron energy is calculated for a hydrogen atom which is placed at an arbitrary position. We adopt a coarse-grid spacing δX of 0.2 bohr and a cut-off radius r_c of 0.928 bohr in the condition that $V_v^{(\text{hard})}(r_c)$ becomes less than 1.0×10^{-4} . Figure 2 illustrates the total energy in which the hydrogen atom is positioned along the center line between coarse-grid points as shown in the inset. Without using the DG technique, the total energy fluctuates depending on the distance between the nucleus position and the coarse-grid points. On the other hand, the DG technique gives stable total energy for any position of the hydrogen atom, and the stability is enhanced by a large value of n_d . In figure 3, where the hydrogen atom is

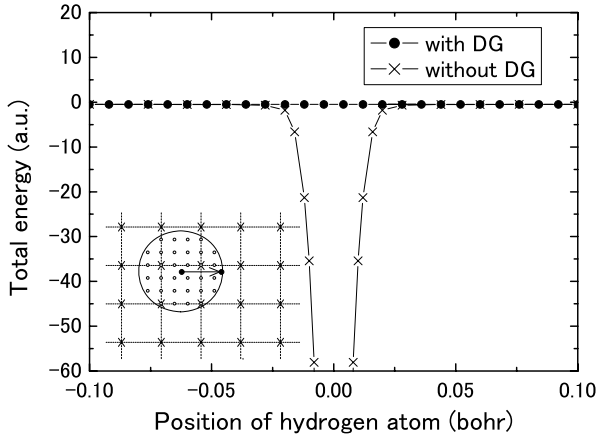


Figure 3. Variation of the total energy of the hydrogen atom as a function of the position of the nucleus. The coarse-grid spacing δX is 0.2 bohr. The hydrogen atom is positioned along the straight line near the coarse-grid points shown in the inset, in which the coarse- and the dense-grid points are indicated by crosses and open circles, respectively. The number of dense-grid points per coarse-grid spacing, n_d , is 25. The result without using the DG technique is also illustrated for comparison. Good stability of the DG technique can be seen.

positioned along the line near coarse-grid points, the calculated total energies without the DG technique show a more intensive fluctuation than in figure 2. It is concluded that the DG technique keeps the total energy stable independent of the position of the hydrogen atom.

5. Example: hydrogen molecule

As an example of the proposed scheme for practical calculations, the adiabatic potential curve of the hydrogen molecule, which is a simple system consisting of two electrons [33, 34], is estimated. The ground state is a singlet one, which is symmetric with respect to coordinates \mathbf{r}_1 and \mathbf{r}_2 [31]:

$$\Psi(\mathbf{r}_1, \mathbf{r}_2) = \sum_{A=1}^L [\phi_1^A(\mathbf{r}_1)\phi_2^A(\mathbf{r}_2) + \phi_2^A(\mathbf{r}_1)\phi_1^A(\mathbf{r}_2)]. \quad (40)$$

The DEM calculations are performed with 64 coarse-grid points along the μ axis and a grid spacing $\delta\mu$ of 0.2 bohr, where μ denotes x , y , or z , and $n_d = 25$ is adopted. A single Slater determinant is applied and the kinetic energy term is calculated using the central-finite-difference formula [25, 26]. In the DEM procedure with the SD method, the iteration is terminated when the sum of the norms of the residual-vectors becomes less than 1.0×10^{-6} . In preliminary calculations using random values as initial wavefunctions, it was confirmed that the wavefunctions converge to states localized near the hydrogen atoms. These localized states are then adopted as initial wavefunctions in the present calculations in order to reduce the number of iterations.

Figure 4 illustrates the calculated ground-state energy for the hydrogen molecule with respect to the interatomic distance by employing the DG technique. The equilibrium

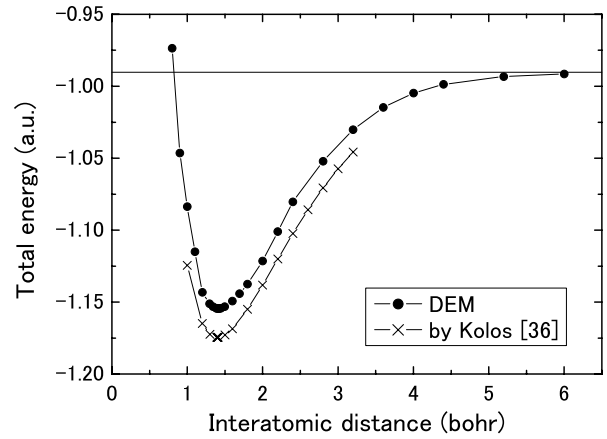


Figure 4. Calculated total energy of the hydrogen molecule as a function of the interatomic distance by the DEM procedure employing the DG technique. The number of coarse-grid points is 64 and n_d is 25, and a coarse-grid spacing δX of 0.2 bohr is adopted. A single Slater determinant is employed. The exact result by Kolos and Wolniewicz is also indicated (\times) [36].

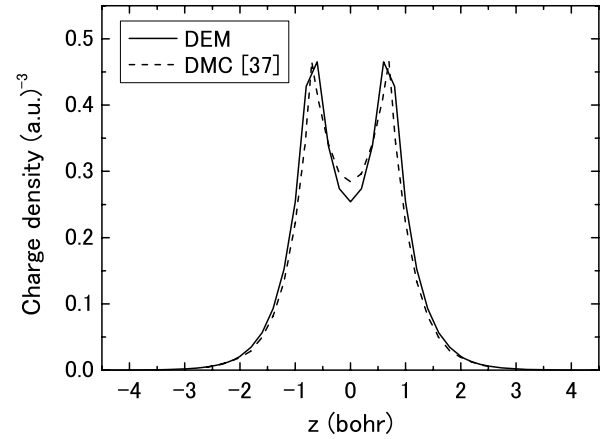


Figure 5. Comparison of the charge density distribution along the molecular axis of the hydrogen molecule evaluated at 1.401 bohr of the interatomic distance between the present result (DEM) and that of the diffusion Monte Carlo (DMC) study by Hongo *et al* [37]. The computational condition is the same as in figure 4.

interatomic distance of 1.416 bohr is obtained with a total energy of -1.15448 au, and it decreases to -1.16141 au in the case of two Slater determinants, in agreement with the exact results reported by Kolos and Wolniewicz: 1.401 bohr and -1.17448 au, which agree with the experimental ones [36].

Comparison of the charge density distribution along the molecular axis of the hydrogen molecule, evaluated at 1.401 bohr, of the interatomic distance between the present result obtained by the DEM and that of the diffusion Monte Carlo (DMC) study by Hongo *et al* is shown in figure 5. As the employed grid spacing (0.2 bohr) is large, the indicated curve by the DEM is not sufficiently smooth compared to that by the DMC. However, it can be thought that these results are acceptable even when a single Slater determinant is adopted. For higher-accuracy computations, many Slater determinants should be employed.

6. Conclusions

A simple and practical method of the search for ground states of few-electron systems has been presented on the basis of the RSFD scheme [25, 26]. As a many-electron wavefunction, a linear combination of Slater determinants is employed, and the total-energy functional is described with overlap integrals of one-electron orbitals.

The ground-state search is performed by applying the DEM procedure to the total-energy functional without the constraints of orthogonality and normalization on the one-electron basis set. For a practical use of the present method, a simple and accessible description of the SD algorithm is presented.

For high-accuracy descriptions of ionic systems, the DG technique [34, 35] is employed. A simple formulation for dealing with systems including nuclei is expressed, and successful results in which the numerical calculation errors caused by the RSFD method are removed by the DG technique are illustrated.

As a practical example of the present method, calculations for the ground-state energy of the hydrogen molecule are demonstrated. An adiabatic potential curve is shown and the accuracy of the calculated result is discussed. The equilibrium interatomic distance and the total energy obtained are in good agreement with the exact results [36, 37].

As a further development of the present scheme, calculations employing appropriate localized basis sets [27, 28, 30] will be made in a future study so as to reduce computational workloads to be linearly proportional to the number of electrons.

Acknowledgments

The present study was supported by Grants in Priority Areas for Scientific Research in the areas of ‘Development of new quantum simulators and quantum design’ (grant No 17064012), ‘Carbon nanotube nano-electronics’ (grant No 19054009) and Global COE Program ‘Center of Excellence for Atomically Controlled Fabrication Technology’ (grant No H08) from the Ministry of Education, Culture, Sports, Science, and Technology (MEXT) of Japan.

References

- [1] Kohn W and Sham L S 1965 *Phys. Rev. A* **140** 1133
- [2] Anisimov V I, Zaanen J and Anderson O K 1991 *Phys. Rev. B* **44** 943
- [3] Solov'yev I V, Hamada N and Teraura K 1996 *Phys. Rev. B* **53** 7158
- [4] Aryasetiawan F and Gunnarsson O 1994 *Phys. Rev. B* **49** 7219
- [5] Georges A and Kotliar G 1992 *Phys. Rev. B* **45** 6479
- [6] Umezawa N and Tsuneyuki S 2004 *Phys. Rev. B* **69** 165102
- [7] Sakuma R and Tsuneyuki S 2006 *J. Phys. Soc. Japan* **75** 103705
- [8] Nazarov V U, Pitarke J M, Takada Y, Vignale G and Chang Y C 2007 *Phys. Rev. B* **76** 205103
- [9] Yamamoto S, Fujiwara T and Hatsugai Y 2007 *Phys. Rev. B* **76** 165144
- [10] Higuchi M and Higuchi K 2007 *Phys. Rev. A* **75** 042510
- [11] Higuchi M and Higuchi K 2007 *Phys. Rev. B* **75** 195114
- [12] Kusakabe K, Suzuki N, Yamanaka S and Yamaguchi K 2007 *J. Phys.: Condens. Matter* **19** 445009
- [13] Kusakabe K 2007 *J. Phys.: Condens. Matter* **19** 365229
- [14] Ohno K, Noguchi Y, Yokoi T, Ishii S, Takeda J and Furuya M 2006 *ChemPhysChem* **7** 1820
- [15] Arita R, Lukoyanov A V, Held K and Anisimov V I 2007 *Phys. Rev. Lett.* **98** 166402
- [16] Kotani T and Akai H 1998 *J. Magn. Magn. Mater.* **177–181** 569
- [17] Akai H and Kotani T 1999 *Hyperfine Interact.* **120/121** 3
- [18] Umrigar C J, Nightingale M P and Runger K J 1993 *J. Chem. Phys.* **99** 2865
- [19] White S R 1992 *Phys. Rev. Lett.* **69** 2863
White S R 1993 *Phys. Rev. B* **48** 10345
- [20] Otsuka Y and Imada M 2006 *J. Phys. Soc. Japan* **75** 124707
- [21] Aimi T and Imada M 2007 *J. Phys. Soc. Japan* **76** 084709
- [22] Kojo M and Hirose K 2008 *Surf. Interface Anal.* **40** 1071
- [23] Maezono R, Ma A, Towler M D and Needs R J 2007 *Phys. Rev. Lett.* **98** 025701
- [24] Maezono R, Watanabe H, Tanaka S, Towler M D and Needs R J 2007 *J. Phys. Soc. Japan* **76** 064301
- [25] Chelikowsky J R, Troullier N, Wu K and Saad Y 1994 *Phys. Rev. B* **50** 11355
- [26] Hirose K, Ono T, Fujimoto Y and Tsukamoto S 2005 *First-Principles Calculations in Real-Space Formalism* (London: Imperial College Press)
- [27] Mauri F, Galli G and Car R 1993 *Phys. Rev. B* **47** 9973
- [28] Mauri F and Galli G 1994 *Phys. Rev. B* **50** 4316
- [29] Hirose K and Ono T 2001 *Phys. Rev. B* **64** 085105
- [30] Sasaki T, Ono T and Hirose K 2006 *Phys. Rev. E* **74** 056704
- [31] Goto H, Yamashiki T, Saito S and Hirose K 2008 *J. Comput. Theor. Nanosci.* at press
- [32] Blaizot J P and Ripka G 1986 *Quantum Theory of Finite Systems* (Cambridge, MA: MIT Press)
- [33] Szabo A and Ostlund N S 1982 *Modern Quantum Chemistry: Introduction to Advanced Electronic Structure Theory* (London: Macmillan)
- [34] Ono T and Hirose K 1999 *Phys. Rev. Lett.* **82** 5016
- [35] Ono T and Hirose K 2005 *Phys. Rev. B* **72** 085115
- [36] Kolos W and Wolniewicz L 1965 *J. Chem. Phys.* **43** 2429
Kolos W and Wolniewicz L 1965 *J. Chem. Phys.* **49** 404
- [37] Hongo K, Kawazoe Y and Yasuhara H 2007 *Int. J. Quantum Chem.* **107** 1459